Developmental Cell, Volume *26*

Supplemental Information

Aurora B and Cyclin B Have Opposite Effects on the Timing of Cytokinesis Abscission in *Drosophila* Germ Cells and in Vertebrate Somatic Cells

Juliette Mathieu, Clothilde Cauvin, Clara Moch, Sarah J. Radford, Paula Sampaio, Carolina N. Perdigoto, François Schweisguth, Allison J. Bardin, Claudio E. Sunkel, Kim McKim, Arnaud Echard, and Jean-René Huynh

INVENTORY OF SUPPLEMENTAL INFORMATION

SUPPLEMENTAL DATA

Figure S1, related to Figure 1 : Survivin localization in mitosis and rescue experiments

Figure S2, related to Figure 1: *aurB*^{2A43} and *svn*^{PBac2180} polyploid phenotype in the germline and larval brain and Svn structure/function analysis.

Figure S3, related to Figure 2: SvnS125E phenotype depends on the CPC, and does not regulate cell cycle length in the larval neuroblasts.

Figure S4, related to Figure 6: Dynamic localization of cycB-5E during early mitosis.

Figure S5, related to Figure 5: Whole western blot using the pcycB antibody

Figure S6, related to Figure 2: Comparison of the nanos, bam and svn promoters in germ cells

Figure S7, related to Figure 3 and Figure 4: Stem cell mitosis

Movie1_NB_WT, related to Figure 1 and Figure S2: Cell division of a wild type larval neuroblast (L2).

Movie2_NB_mut, related to Figure 1 and Figure S2: Cell division of a *svn*^{PBac2180} homozygous mutant larval neuroblast (L2).

Movie3_GSC_Svn125E, related to Figure 3: Mitosis of a germline stem cell expressing a phosphomimic form of Svn (Svn125E) driven by the *nanos* promoter.

Movie4_CycB5E, related to Figure 6: Stem-cyst made of 4 cells, expressing a phosphomimic form of Cyclin-B tagged with GFP and driven by the *nanos* promoter.

Movie5_PAGFP_CycB5E, related to Figure 6: Germarium with germ cells expressing both a phosphomimic form of Cyclin-B tagged with GFP, and α-tubulin tagged with photoactivable GFP

Movie6_PAGFP_WT, related to Figure 6: Germarium with germ cells expressing α-tubulin tagged with a photoactivable GFP.

Movie7_GSC_SvnWT, related to Figure 3 and Figure 4: Mitosis of a germline stem cell expressing a wild-type form of Svn driven by the *nanos* promoter.

SUPPLEMENTAL EXPERIMENTAL PROCEDURES

Detailed description of the materials and methods used.

SUPPLEMENTAL REFERENCES

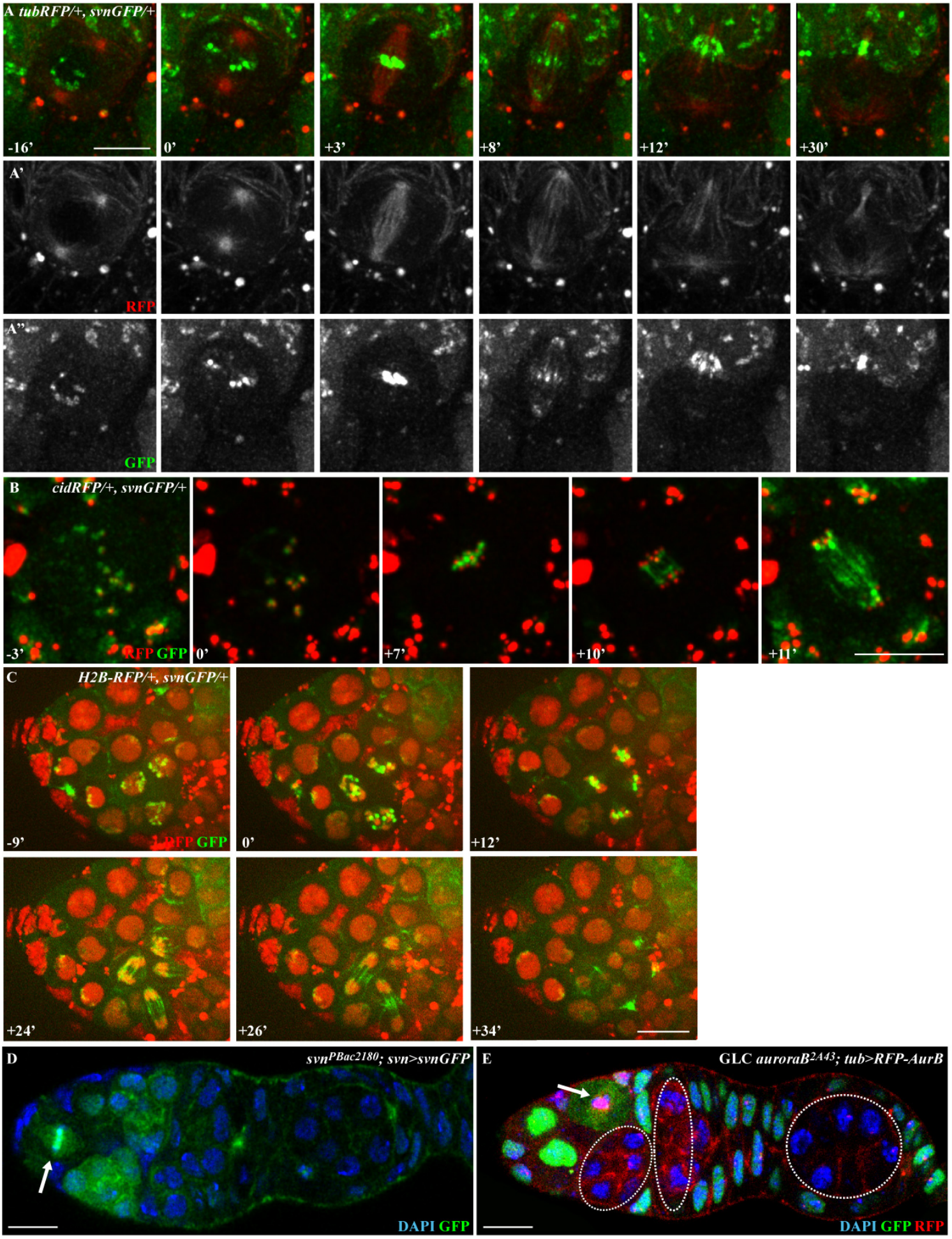
A tubRFP/+, svnGFP/+
-16'
0'
+3'
+8'
+12'
+30'
A'
RFP
A"
GFP
B
cidRFP/+, svnGFP/+
-3'
RFP GFP
0'
+7'
+10'
+11'
C
H2B-RFP/+, svnGFP/+
-9'
RFP GFP
0'
+12'
+24'
+26'
+34'
D
svnPBac2180; svn>svnGFP
DAPI GFP
E
GLC auroraB2A43; tub>RFP-AurB
DAPI GFP RFP

FIGURE S1

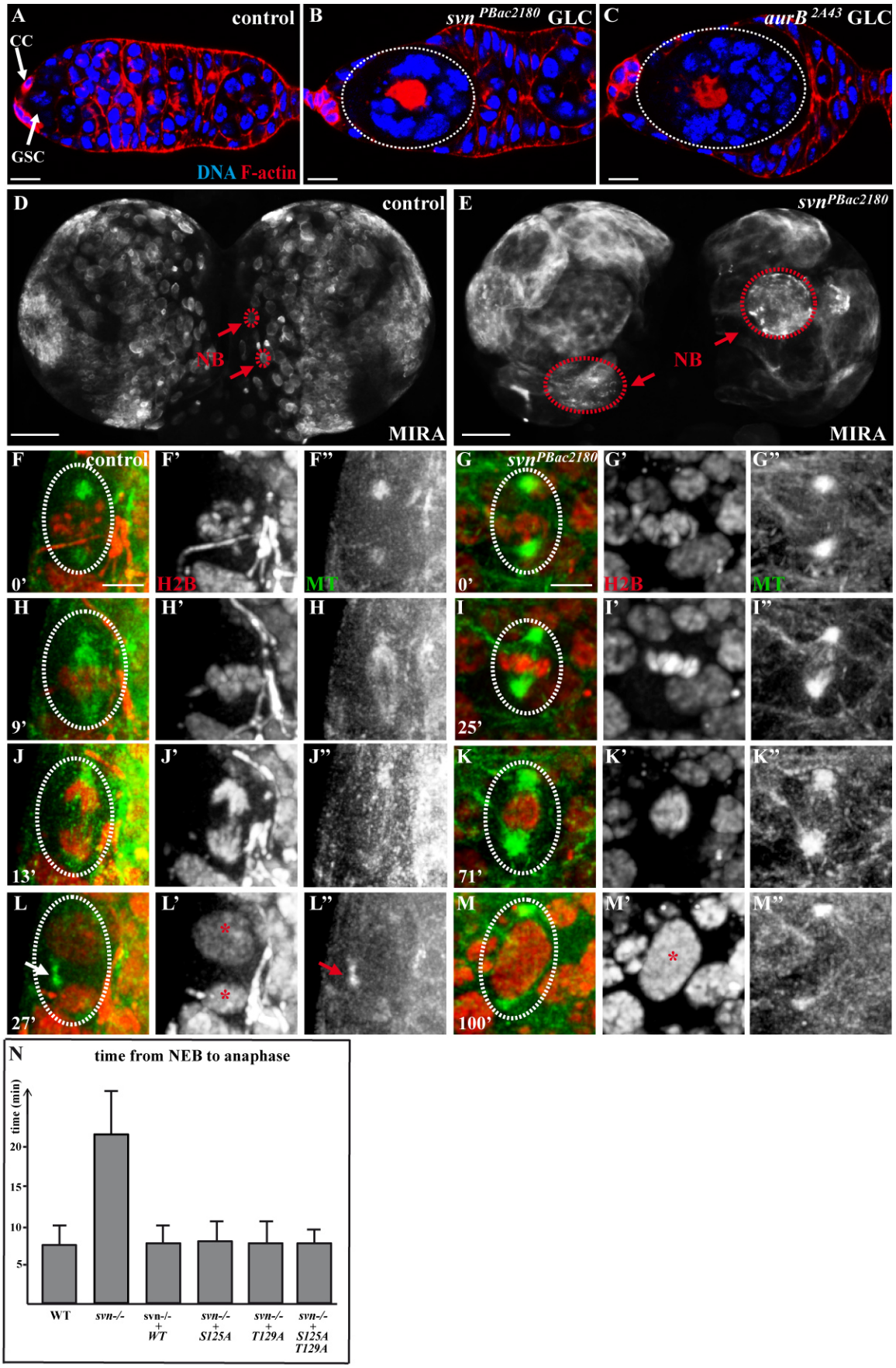
A
control
CC
GSC
DNA F-actin
B
svn PBac2180 GLC
C
aurB 2A43 GLC
D
control
NB
MIRA
E
svnPBac2180
NB
MIRA
F
control
F'
F"
0'
H2B
MT
G
svnPBac2180
G'
G"
0'
H2B
MT
H
H'
H
9'
I
I'
I"
25'
J
J'
J"
13'
K
K'
K"
71'
L
L'
L"
27'
M
M'
M"
100'
N
time from NEB to anaphase
time (min)
5
10
15
20
WT
svn-/-
svn-/- + WT
svn-/- + S125A
svn-/- + T129A
svn-/- + S125A T129A

FIGURE S2

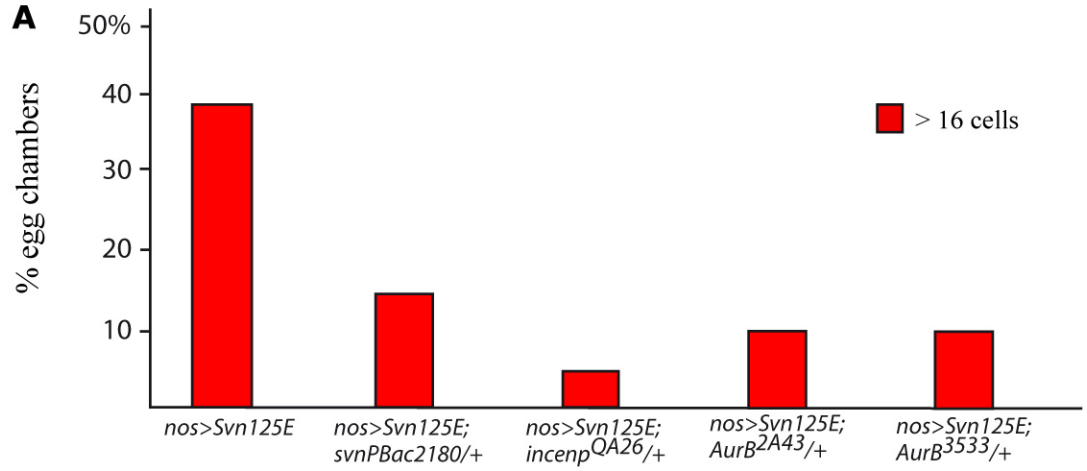
A
50%
40
30
20
10
% egg chambers
> 16 cells
nos>Svn125E
nos>Svn125E; svnPBac2180/+
nos>Svn125E; incenp^QA26/+
nos>Svn125E; AurB^2A43/+
nos>Svn125E; AurB^3533/+

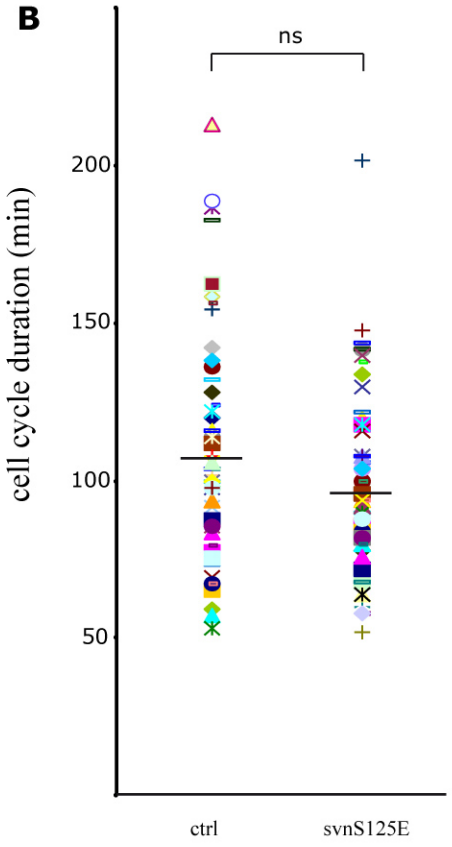
B
ns
200
150
100
50
cell cycle duration (min)
ctrl
svnS125E

Figure S3

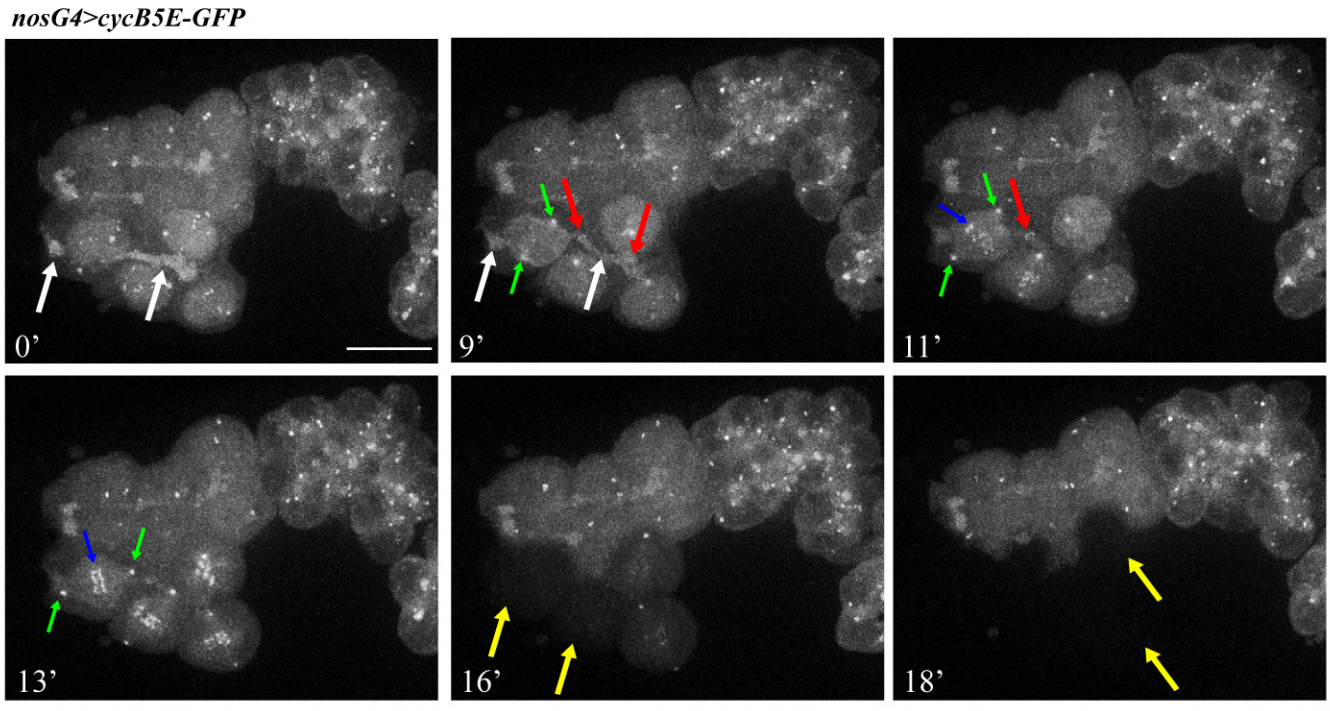
nosG4>cycB5E-GFP
0’
9’
11’
13’
16’
18’

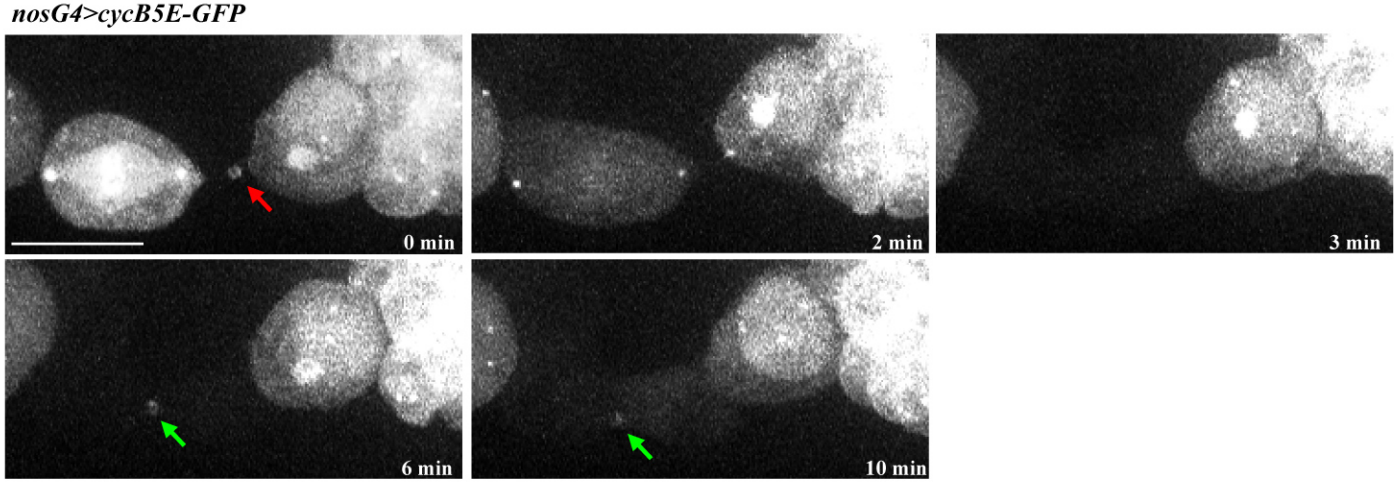
nosG4>cycB5E-GFP
0 min
2 min
3 min
6 min
10 min

Figure S4

A. full blot corresponding to the image presented in figure 5H

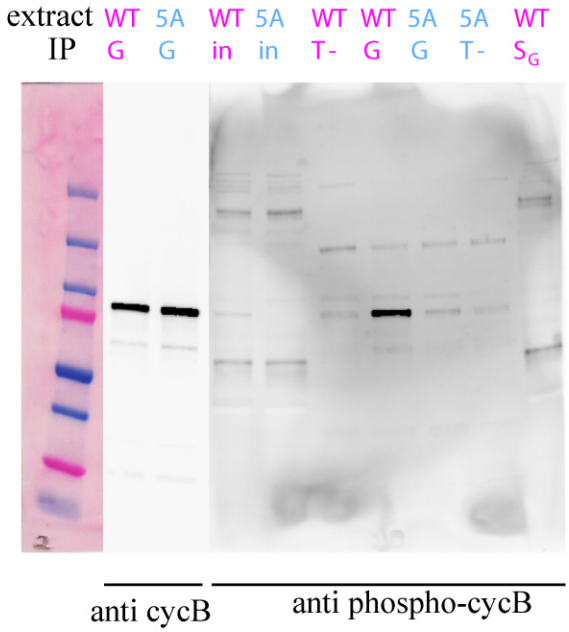

IP G: GFP
in: input
IP T-: control beads
S: supernatent post IP

← cycB-GFP 89 kD

B. full blot corresponding to the image presented in figure 5I

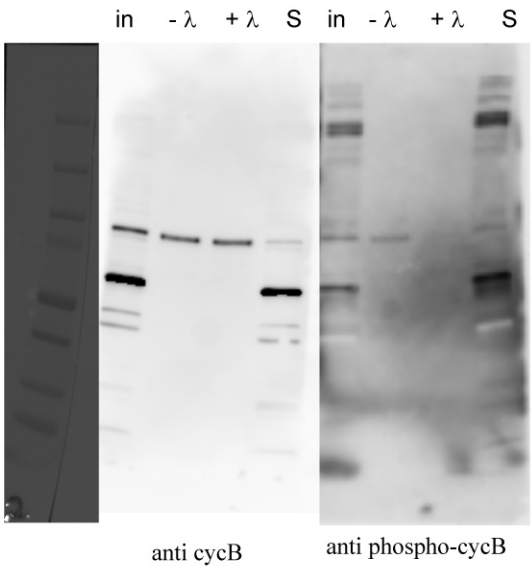

← cycB-GFP 89 kD
← Cycline B endogenous = 59 kD

in: input
S: supernatent post IP

C. full blot corresponding to the image presented in figure 5J

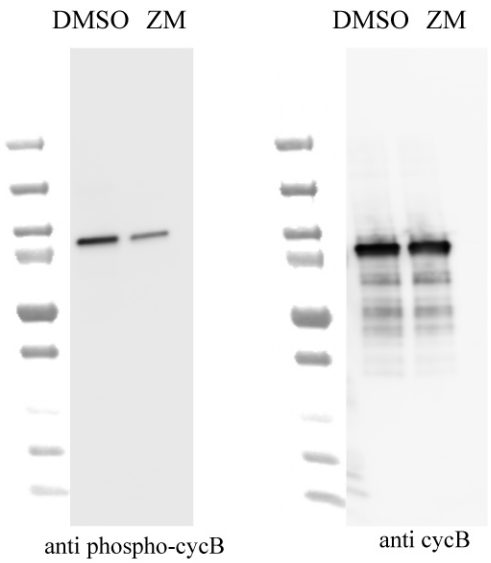

← cycB-GFP 89 kD

Figure S5

Figure S6

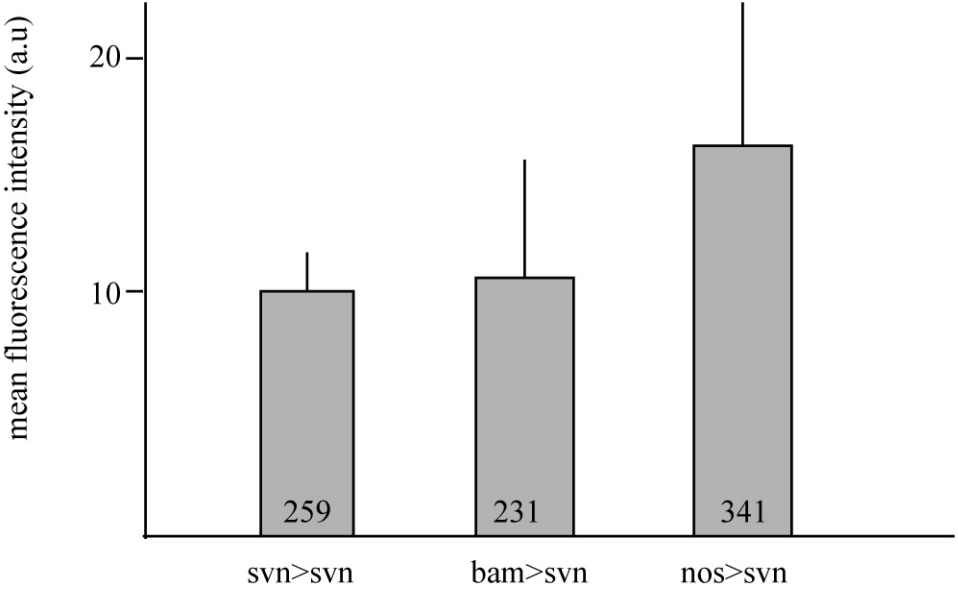
mean fluorescence intensity (a.u)
20
10
259
231
341
svn>svn
bam>svn
nos>svn

Figure S7

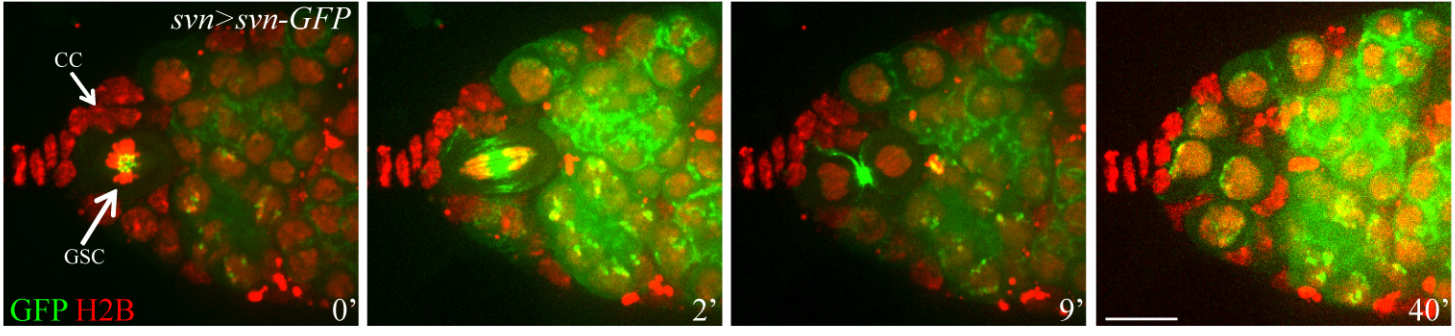

Supplementary figures legends

Figure S1 : Survivin localization in mitosis and rescue experiments, related to Figure 1

(A) Selected projection of Z-sections obtained from time lapse spinning disc microscopy performed on third instar larval brains expressing *svn-GFP* under the control of the *svn* promoter (green in overlay, white in the third row) and *tubulin-RFP* (red in overlay, white in the second row). The time in minutes is indicated at the bottom left, time point 0 is when the nuclear envelope breaks down (NEBD).

(B) Selected projection of Z-sections obtained from time lapse spinning disc microscopy performed on third instar larval brains expressing *svn-GFP* under the control of the svn promoter (green in overlay) and *cid-RFP* (red). The time in minutes is indicated at the bottom left, time point 0 is when the nuclear envelope breaks down. The intensity of the green channel has been increased at tp -3 and tp 11 to highlight Svn-GFP in pericentic region in prometaphase (tp -3), and at the spindle midzone (tp 11).

(C) Selected projection of Z-sections obtained from time lapse spinning disc microscopy performed on germarium of females expressing *svn-GFP* under the control of the *svn* promoter (green) and *H2BRFP* (red). The time in minutes is indicated at the bottom left, time point 0 is when the nuclear envelope breaks down.

(D) Germarium of a svn^{PB2180} homozygous mutant female rescued by *svn-GFP* expressed under the control of the *svn* promoter, stained with DAPI. GFP is in green. Note the strong localization of Svn-GFP at the centromeres in the mitotic cell (arrow).

(E) Germarium of a female harboring $aurB^{2A43}$ germline clones (GLC, marked by the absence of GFP and surrounded white lines) rescued by the expression of *RFP-AurB* under the control of the ubiquitous *tubulin* driver, stained with DAPI. Note the strong localization of Svn-GFP at the centromeres in the mitotic cell (arrow)

Scale bar: 10 μm.

Figure S2: $aurB^{2A43}$ and $svn^{PBac2180}$ polyploid phenotype in the germline and larval brain and Svn structure/function analysis, related to Figure 1.

(A-C) Germaria of WT female (A), or females with $svn^{PBac2180}$ (B) or $aurB^{2A43}$ (C) germ line clones (GLC, surrounded by dotted lines) stained with DAPI (DNA) and Phalloidin (F-actin). Germline stem cells (GSC), with a round spectrosome, are at the anterior tip, attached to the cap cells (CC). One Zsection is shown. Note the enlarged spectrosome in the mutant stem cells.

(D-E) Third instar WT (D) and *svn*^{PBac2180} homozygous (E) larval brains stained with the neuroblast (NB) marker Miranda (MIRA). 2 neuroblasts are encircled by dotted lines in each brain.

(F-M) Selected projection of Z-sections obtained from time lapse spinning disc microscopy performed on second instar larval WT (F, H, J, L) and *svn*^{PBac2180} (G, I, K, M) brains expressing H2B-RFP (middle, and red in overlay) and Tubulin-GFP (right, and green in overlay). The time in minutes is indicated at the bottom left corner. The nuclei resulting from the 2 mitosis are marked by a star. Note the absence of midbody (arrow in WT) in *svn*^{PBac2180} mutant neuroblast.

(N) Timing of prometaphase + metaphase in WT, *svn*^{PBac2180} mutants and in the *svn*^{PBac2180} mutants expressing the different *svn* variants, quantified in larval neuroblasts.

Scale bar: 10 μm in A, B and C, 50 μm in D and E, 5 μm in F and G.

Error bars are SD.

See also Movie 1 and Movie 2.

Figure S3: SvnS125E phenotype depends on the CPC, and does not regulate cell cycle length in the larval neuroblasts, related to Figure 2

(A) Fraction of egg chambers exhibiting more than 16 cells on the Y axis. The rest of the egg chambers have 16 cells. Genotypes are on the X axis. The penetrance of SvnS125E phenotype is decreased by a reduction in the levels of CPC components.

(B) Cell cycle duration of larval neuroblasts measured by live imaging of L3 brains expressing Tubulin-GFP alone (ctrl) or with SvnS125E. The difference observed between the 2 genotypes is not significant (student test).

Figure S4: Dynamic localization of CycB-5E during early mitosis, related to Figure 6.

Top: Selected projection of Z-sections obtained from time lapse spinning disc microscopy performed on a germarium expressing *cyclinB5E-GFP* under the control of the *nanos-Gal4* driver. The time in minutes is indicated at the bottom left. CycB5E is enriched in the nucleus and localizes on the fusome of the stem cyst in early mitosis (white arrows), and later concentrates on the ring canals (red arrows). Like CycBWT, CycB5E localizes at the centrosomes (green arrows) and at the centromeres (blue arrows), and disappears at anaphase onset. Note that the two most anterior cells are in slight advance compared to the two posterior ones: cycB5E accumulates earlier at the poles (9 min, versus 11min), at the centromeres (11 min versus 13 min), and enter anaphase earlier as well (16 min, versus 18 min,

yellow arrows).

Bottom: Selected projection of Z-sections obtained from time lapse spinning disc microscopy performed on a germarium expressing *cycB5E-GFP* under the control of the *nanos-Gal4* driver. A close up of 2 cells of a stem cyst is shown. At 0 min, we note the presence of CycB5E-GFP at the midbody linking the 2 cells (red arrow), the one on the left being in metaphase. At 2 min, the left cell enters anaphase, and CycB5E-GFP gets degraded, fully at 3min. At 6 min, some CycB5E-GFP accumulates at the newly formed midbody (green arrow), still visible at 10min.

Scale bar: 10 μm

Figure S5: Whole western blot using the p-CycB antibody, related to Figure 5

(A) Full blot corresponding to the image presented in figure 5H.

(B) Full blot corresponding to the image presented in figure 5I.

(C) Full blot corresponding to the image presented in figure 5J.

Figure S6: Comparison of the nanos, bam and svn promoters in germ cells, related to Figure 2.

Quantification of the fluorescence intensity (arbitrary unit, a.u.) in interphase germ cells expressing either svn-GFP under the control of svn promoter (left), bam-gal4 driver (middle), or nanos-gal4 driver (right).

Error bars are SD.

Figure S7: Stem cell mitosis, related to Figure 3 and Figure 4

Selected projection of Z-sections obtained from time lapse spinning disc microscopy performed on a $svn^{PBac2180}$/+ germarium expressing ubiquitously *H2B-RFP* and *svn-GFP* under the control of *svn* promoter. The time in minutes is indicated at the bottom left. At 0min, a single germline stem cell (GSC) is in metaphase, attached to Cap cells (Cc). It enters anaphase at 2min, and cytokinesis at 9 min. Note that only one GSC is in mitosis, no neighboring GSC undergoes mitosis synchronously in region 1 during the 40 minutes of the movie.

Scale bar: 10 μm

MOVIES LEGENDS

Movie1_NB_WT, related to Figure S2: Cell division of a wild type larval neuroblast (L2). In Green is the protein-trap line G147 which labels the microtubules. In Red is Histone2BRFP. Projection of a Z-stack is shown.

Movie2_NB_mut, related to Figure S2: Cell division of a $svn^{PBac2180}$ homozygous mutant larval neuroblast (L2). In Green is the protein-trap line G147 which labels the microtubules. In Red is Histone2B-RFP. Chromosomes alignment on the metaphase plate is delayed compared to wild type. The nuclear envelope reforms before chromosomes are well separated. There is no formation of midbody. The resulting neuroblast is polyploidy. Projection of a Zstack is shown.

Movie3_GSC_Svn125E, related to Figure 3: Mitosis of a germline stem cell expressing a phosphomimic form of Svn (Svn125E) driven by the *nanos* promoter. In Green is Svn125EGFP and in Red is Histone2B-RFP. The GSC (arrow GSC) can be identified by its strong adhesion to the somatic cells of the niche (arrow Cap). This GSC simultaneously with 3 other neighboring cells. Note that Svn125E localization and dynamics are similar to wild type Svn (Movie7). Projection of a Z-stack is shown.

Movie4_CycB5E, related to Figure 6: Stem-cyst made of 4 cells, expressing a phosphomimic form of Cyclin-B tagged with GFP and driven by the *nanos* promoter. Cyclin-B localizes on the spectrosome/fusome, on centrioles and transiently on kinetochores and ring canals before being mostly degraded at anaphase. Projection of a Z-stack is shown.

Movie5_PAGFP_CycB5E, related to Figure 6: Germarium with germ cells expressing both a phosphomimic form of Cyclin-B tagged with GFP, and α-tubulin tagged with photoactivable GFP. One GSC appears Green with high levels of CycB5E-GFP and is probably in G2 phase. A neighboring GSC appears dark and is probably in G1 phase. The red circle marks the region activated by a 2-photon laser. Upon activation at 820nm tubulin-PAGFP becomes green and the fluorescence quickly diffuses to the two neighboring cells

(labeled 1 and 2), indicating that all three cells are physically linked. Cell 1 is then also activated and the fluorescence becomes evenly distributed within the stem-cyst, including Cell 2 (GSC) which has never been directly activated. There is also a third activation of Cell 3 in which the fluorescence had also diffused. All four cells are thus physically linked. Projection of a Z-stack is shown.

Movie6_PAGFP_WT, related to Figure 6: Germarium with germ cells expressing α-tubulin tagged with a photoactivable GFP. The red circle marks the region activated by a 2-photon laser. Upon activation at 820nm Tubulin-PAGFP becomes green. The fluorescence accumulates in the GSC after each activation, indicating that the GSC is not physically linked to any other cell. Projection of a Z-stack is shown.

Movie7_GSC_SvnWT, related to Figure 3 and Figure 4: Mitosis of a germline stem cell expressing a wild-type form of Svn driven by the nanos promoter. In Green is Svn125E-GFP and in Red is Histone2B-RFP. The GSC can be identified by its strong adhesion to the somatic cells of the niche. Projection of a Z-stack is shown. Control experiment of Movie3.

SUPPLEMENTAL EXPERIMENTAL PROCEDURES

Fly Strains

We screened a collection PBac insertions generated on FRT chromosomes during a genetic screen for border cells migration defects during *Drosophila* oogenesis (Mathieu et al, 2007). We used the FLP/FRT system to induce homozygous mutant clones (mainly in the germline), and screened for early arrest of oogenesis. *PBac2180* insertion induced highly polyploidy cells. The insertion site of *PBac2180* was identified by inverse PCR and sequencing (Hacker et al., 2003), and *PBac2180* was found to be located in the regulatory sequences of the deterin/survivin (svn)locus. Another allele of *svn*, *PBac1527*, also inserted in the regulatory region of svn, was obtained at the Bloomington Stock Center. Homozygous individuals, as well as trans-heterozygous of these two *svn* alleles, or trans-heterozygous of a PBac over a deficiency of the region could survive until pupal stage. Mutations in *aurB* were generated during two independent EMS mutagenesis and screens. These mutations induced highly polyploid cells, which were very reminiscent of *PBac2180* mutant clones. In the first screen, MARCM clones were induced for mutagenized chromosomes on chromosome 2L, and adult gut stem cells were analyzed (Lee and Luo, 2001; Perdigoto et al., 2011). The *2A43* allele induced highly polyploidy cells and early arrest of oogenesis. It was mapped with deficiencies to a small interval containing 3 genes, including the *aurB* candidate. The mutation was then identified by direct sequencing of the *aurB* locus. The second screen was performed to identify mutations, which were synthetic lethal with subito. The *1689* and *3533* and *2A43* alleles were found to be part of the same complementation group. In all three alleles, mutations in *aurB* were identified by sequencing homozygous mutant genomic DNA. All fly cultures were performed at 25°C. w^{1118} was used as control strain. The following alleles and transgenes were used: $bam^{\Delta 86}$ (Bopp et al., 1993); hts^{1} (Yue and Spradling, 1992); hts^{01103} (Spradling et al., 1999) ,$encore^{R1}$ (Hawkins et al., 1996), $cycB^{2}$ and $cycB^{3}$(Jacobs et al., 1998); $cycB^{KG08886}$ (Bloomington Stock Center); Df(3L)A466 (Hawkins et al., 1996); *hs-bam* (Li et al., 2009); *UAS-PA-GFP* (Murray and Saint, 2007); *UAS-Trip cycB* (Ni et al., 2011) ;

Ubq-RFP-α-Tubulin (Basto et al., 2008); *cid-RFP* (Schuh et al., 2007), *H2B-RFP* (Schuh et al., 2007)and *jupiter-GFP* (Karpova et al., 2006).

The germline clones were generated using the FLP/FRT technique (Chou and Perrimon, 1992) (Xu and Rubin, 1993) using a nlsGFP recombined onto FRT40A, or FRT82B (Bloomington Stock Center). Clones were induced by heat-shocking third instar larvae at 37°C for 2 hours. Overexpression experiments were performed using the Gal4/UASp system (Brand and Perrimon, 1993) with the *nanos-Gal4* (Van Doren et al., 1998) or the *bam-Gal4* (Chen and McKearin, 2003) drivers. Quantification of the percentage of egg chambers having more or less than 16 cells were done on one day old females because we noticed a decrease in the penetrance of the phenotype with age.

Cell culture, transfection and drug treatments

HeLa cells (CCL-2 from ATCC) were cultured at 37°C, 5% CO2 in DMEM (Gibco) supplemented with 10% FBS. MEF *cyclinB2* +/+ and -/- (Brandeis et al., 1998) were given by J. Sobczak-Thepot and cultured like HeLa cells.

HEK 293T cells were cultured at 37°C, 5% CO2 in DMEM (Gibco) supplemented with 10% FBS + 1% L-Glutamin + 1% MEM (Non-essential Amino Acid Solution) + 1% Penicillin/Streptomycin.

Transfection of ATCC cells were performed using FuGENE-6 (Roche) according to Manufacturer's instructions. The plasmid endoding myc-CycB2-GFP was obtained from J.Sobczak-Thepot. Plasmids were transfected for 48hrs before immunostainning.

HEK 293T (2.10^6) cells were transfected by the plasmids pCMV-HA-AurB and/or pCMVcycB-GFP (4 μg total) using PEI (Polyethylenimine).

Cells have been treated with 2 μM ZM447439 (TOCRIS Bioscience) and/or with 300 nM cdk1/2 inhibitor III (Merk).

Constructs and Antibodies

To generate the genomic rescue construct of *survivin*, a PCR fragment corresponding to the

survivin locus (promoter + gene region until the last codon except the STOP) was amplified from genomic DNA using the primers 5'ACTAGTGAAACAGCTGCTGTAACAGACG 3' and 5'GGTACCTTTTTGATTACGCGTAAACTCA 3' and cloned into the INVITROGEN pCRII-TOPO vector (pCRII:svn); a PCR fragment corresponding to eGFP coding sequence was amplified with the primers 5'GGTACCATGGTGAGCAAGGGCGAGGAGC 3'and 5'GAATTCTTACTTGTACAGCTCGTCCATG 3'and cloned into pCRII-TOPO ;
a last fragment corresponding to survivin 3'UTR was amplified with the primers 5'TAGAGCGCTAATTTTTAAACC 3' and 5'GAATTCCCTATTACAGTTTAATTTATAAATACATTC 3' and cloned into pCRIITOPO.
All three fragments were sequenced and subcloned into pCASPER4 to get the fusion protein survivin tagged by eGFP in C-terminal and expressed under the control of its own promoter (pCasper: svn>svnGFP).
To generate the svn>svnΔBIR construct, two PCR fragments of survivin flanking the BIR domain were amplified on pCasper: svn>svnGFP using the primers pairs 5'ACTAGTGAAACAGCTGCTGTAACAGACG 3' and 5'GAATTCACGCGATGCTGTTCCAGGAGG 3' as well as 5'GAATTCCCCCAATGCGAGTTCGCCAAGC 3' and 5'GGTACCTTTTTGATTACGCGTAAACTCA 3'¦. Both fragments were subcloned in frame into pCasper: svn>svnGFP deleted of the original svn fragment to generate pCasper: svn>svnΔBIR-GFP.
Point mutations in the Survivin coding sequence (C97A, S125A and T129A) were generated by PCR on pCRII:svn with the GeneTailor Site-Directed mutagenesis System (Invitrogen) using the following primers pairs:
5'ACGTGAAACATGCACCCCAAGCCGAGTTCGCCAA 3' and 5'TTGGGGTGCATGTTTCACGTGCTCCTTCCA 3' for C97A;
5'TTGGAACCGTCGTTAAAGGCGCCATAGAGAAAAC 3'and 5'GCCTTTAACGACGGTTCCAAGAATTTCCAG 3' for S125A;
5'TTAAAGGCAGCATAGAGAAAGCCTGCAAAGCCTT 3' and

5’TTTCTCTATGCTGCCTTTAACGACGGTTCC 3’ for T129A.

The mutations were checked by sequencing, and the svn mutant fragments were subcloned into pCasper: svn>svn-GFP deleted of the original svn fragment.

Double S125A+T129A point mutations in the Survivin coding sequence was generated by adding the T129A mutation on the pCRII:svnS125A plasmid, using the same mutagenesis system, by PCR with the primer pair:

5’TTAAAGGCGCCATAGAAAAAGCCTGCAAAGCCTT 3’ and

5’TTTTTCTATGGCGCCTTTAACGACGGTTCC 3’

The mutations were checked by sequencing, and the svn double-mutant fragment was subcloned into pCasper: svn>svn-GFP deleted of the original svn fragment.

To generate the UASp>svnWT-GFP transgene, a DNA fragment was amplified on pCasper: svn>svnGFP with the primers 5’CACAGCAACAACGACGCGCTGTTTGCG 3’ and 5’CCTATTACAGTTTAATTTATAAATACATTC 3’, cloned into pCRII-TOPO, sequenced, and subcloned into pUASp1.

To generate the UASp>svn125E-GFP transgene, S125E phosphomimic point mutation in the Survivin coding sequence was generated with the same mutagenesis system, by PCR on pCRII:svn plasmid with the primer pair:

5’TTGGAACCGTCGTTAAAGGCGAGATAGAAAAAAC 3’ and

5’GCCTTTAACGACGGTTCCAAGAATTTCCAG 3’

The mutation was checked by sequencing, and the svn mutant fragment was subcloned into pUASp>svnWT-GFP deleted of the original svn fragment.

To generate the tub>RFP-aurB rescue construct, two PCR fragments were amplified on mRFP plasmid (pPWR) and on genomic DNA with the following primers:

5’CCGGATCCATGGCCTCCTCCGAGGACGTCATCAA 3’ and

5’CCGGTACCGGCGCCGGTGGAGTGGCGGCCCTCGG 3’ for mRFP;

5’CCGGTACCATGACGCTTTCCCGCGCGAAGCACGC 3’ and

5’CCGAATTCCTCCAAACTTCATTAAATCTTATAAACCG 3’ for aurB. Both fragments were subcloned in frame in pBluscript and sequenced. The fusion fragment was subcloned into pCasper-tub to generate a pCasper: tub>RFP-aurB construct.

To generate the UAS-HA-aurB transgene, the coding region of AurB was amplified from cDNA LD39409 and then cloned into the Gateway pENTRTM4 vector (Invitrogen). An LR 'clonase' reaction was then performed to recombine aurB into the ppHW destination vector (Invitrogen) that contains 3 copies of an N-terminus HA-tag under the control of an inducible UASp promoter.

To generate the pUASp>RFP-aurA transgene, a PCR fragment corresponding to the whole aurora A genomic coding region (from the START until the last codon except the STOP) was amplified from genomic DNA using the primers 5'CACCATGTCCCATCCGTCTGACC 3' and 5'CTGCGTGTGCGCCAGGATCC 3' and cloned into the pENTR/D-TOPO Gateway entry vector using the pENTR directional TOPO cloning kit (Invitrogen). The aurA gene was then transferred by LR recombination using the Gateway LR clonase II enzyme mix (Invitrogen) to pPRW destination vector (obtained from Terence Murphy's laboratory Drosophila Gateway Vector Collection at Carnegie Institution.

To generate the pUASp>CycB-WT-GFP transgene, a PCR fragment corresponding to the whole-length Cyclin-B cDNA (isoform A, from the START until the last codon except the STOP) was amplified from a pKS-CycB plasmid (kindly provided by Jordan Raff), using the primers 5'CACCATGGTGGGCACAACACTG 3' and 5'TTTCCTCTGGCTCTGGCCC 3' and cloned into the pENTR/D-TOPO Gateway entry vector (pENTR-CycB). The cycB cDNA was then transferred by LR recombination to pPWG destination vector (obtained from Terence Murphy's laboratory Drosophila Gateway Vector Collection).

To generate the pUASp>CycB-5A-GFP (non-phosphorylatable form of the five potential Aurora-B phosphorylation sites) and pUASp>CycB-5E-GFP (phosphomimic form of the five same sites) transgenes, point mutations of the first potential site (T27) were first generated with the same mutagenesis system, by PCR on pENTR-CycB plasmid, using the following primers pairs:

5'AAGTGCAATTGAAGAAATTGGCGGTTCCTTCCATG 3' and

5'CAATTTCTTCAATTGCACTTGCTTGAAGTTC "' to obtain pENTR-CycB-T27A ;

5'AAGTGCAATTGAAGAAATTGGAGGTTCCTTCCATG 3' and

5'CAATTTCTTCAATTGCACTTGCTTGAAGTTC 3' to obtain pENTR-CycB-T27E.

Two different small DNA fragments, encompassing the remaining four potential sites, were synthesized by MWG : fragment 4A (leading to non-phosphorylable mutation of amino-acids T124A+T125A+T132A+S157A+S200A) and fragment 4E (leading to phosphomimic mutation of amino-acids T125E+T132E+S157E+S200E). These 4A and 4E fragments were then subcloned into pENTR-CycB-T27A and pENTR-CycB-T27E respectively, deleted of the original wild-type fragments, to obtain pENTR-CycB-5A and pENTR-CycB-5E respectively. Finally, both Cyclin B mutated forms were transferred by LR recombination to pPWG destination vector, leading to the final pUASp>CycB-5A-GFP and pUASp>CycB-5E-GFP transgenes.

All transgenic lines were generated by the BestGene Inc, except UASp>HA-AurB for which the construct was injected into fly embryos by Model System Genomics at Duke University.

Generation of the Anti-pS157-CycB antibody:

A phosphorylated Cyclin B peptide, SNLS**KKS$_{157}$(PO3H2)L**TKLR, corresponding to the 4th potential Aurora-B phosphorylation site, was synthesized and used for immunization of two rabbits in a 28-day fast protocol (Eurogentec). Both resulting crude polyclonal sera were mixed and the phospho-specific antibodies were then double-purified by Eurogentec, first using an affinity column with the immunization phosphorylated peptide, and then the eluted fraction was counter-selected against another column containing the corresponding nonphosphorylated peptide. Dot Blot analysis of the purified antibody showed a specificity about 30 times better for the phosphorylated peptide than for the non-phosphorylated one. The final purified antibody was used at 1:1,000 for Western Blots.

Immunohistochemistry in flies and cells

Antibody staining and Hoechst staining were performed according to standard protocols. Briefly, ovaries were dissected in PBS, fixed in 4% PFA, permeabilized in PBT (PBS-0,2%Triton) for 30 min, left overnight with primary antibodies in PBT at 4°C, washed 2 h in PBT, left with secondary antibody for 2 hrs at room temperature, washed 1 h in PBT and mounted in Cityfluor.

Cells were fixed on ice in 10% TCA for 20 min, and rinsed in PBS. They were then permeabilized in PBS-5% BSA-0,1% Triton for 3 min, and blocked in PBS-5% BSA 10 min. Primary antibodies were applied in PBS-5% BSA was followed by 3 washes in PBS-5% BSA for 1 hr. After 3 washes in PBS-5% BSA, a 30 minutes secondary antibodies incubation was performed, followed by a DAPI wash (1:2000 in PBS-5% BSA) and 2 regular washes. Coverslips were mounted in Mowiol before observation.

The primary antibodies used in flies were the following: mouse-anti-α-spectrin (clone 3A9, DSHB) 1:500; rb anti-α-spectrin 1:1000 (Byers et al., 1987), rat-anti-BamC 1:1000 (McKearin and Ohlstein, 1995) ; rb-anti-Nanos 1:200 (Hanyu-Nakamura et al., 2004); rb-anti-pSMAD1:100 (a king gift of Peter ten Dijke); rb-anti pH3S10 1:1000 (Upstate); rb-anti-INCENP 1:500 (Adams et al., 2001); rat-anti-INCENP 1:1000; rb-anti-AurB 1:50 (Giet and Glover, 2001); rat-anti-CID 1:1500 (Martins et al., 2009) ; mouse-anti-α-tubulin 1:500 (Sigma, clone DM1A), and mouse-anti-α-tubulin-FITC 1:500 (Sigma, clone DM1A).

The primary antibodies used in cells were the following: rabbit anti- mouse cyclinB2 (Brandeis et al., 1998), a kind gift of Mark Carrington (Cambridge University), used at 1:100, and human anti-α-tubulin (F2C, gift from F. Perez, Institut Curie, Paris, France, (Nizak et al., 2003)) used at 1:500.

Fluorescent secondary antibodies were from Jackson Immunoresearch; rhodamin-phalloidin and DAPI were from Molecular Probes.

For EdU treatment (Click-iT Edu Imaging kit, Invitrogen), ovaries were dissected in Schneider medium complemented with 10% FBS. There were then incubated at 25°C for 30 min in 20 μM EdU in Schneider medium+ 10% FBS. Edu detection was performed according to Manufacturer's instructions.

For orcein staining of larval brains, brains were dissected in 0.7% NaCl, and submitted to a hypotonic choc of NaCi 1% for 5 min. They were then incubated 15 sec in acetic acid 45%, followed by 30 sec in acetic acid 60%. Brains were then incubated 1 min in a drop of acetoorcein 2% on a coverslip, and subsequently squashed.

Immunoprecipitation, Western Blotting

For the blot of figure 3, denatured ovary extracts were fractionated by SDS-PAGE using 10% gel and electrotransferred to Protran nitrocellulose membranes (Schleicher & Schuell). The membranes were blocked overnight at 4°C in blocking buffer (PBS , 0.1% Tween 20, 5% milk) and incubated for 2 h in the same buffer containing primary antibodies at the following dilutions: anti-GFP at 1/10000 (Ahmed El Marjou, Institut Curie, proteomic platform) and anti-α-tubulin (clone DM1A, Sigma) at 1/5000. After three washes in PBS-T (PBS, 0.1% Tween 20), membranes were incubated for 1 h with the secondary antibody in blocking buffer containing a peroxydase-conjugated anti-rabbit IgG (Jackson Immunoresearch) diluted at 1/10000. After three washes in PBS-T, bands were detected with the SuperSignal West Pico Chemiluminescent Substrate (Pierce) and visualized using a mini-LAS-4000 Imaging System (Fujifilm).

GFP-immunoprecipitation (IP) experiments were performed with 25 µl of magnetic GFPTrap R-M beads (Chromotek) per experimental condition. Beads were first equilibrated by three washes in IP Washing Buffer [50 mM Tris-HCl pH 7.4, 2 mM EDTA, 150 mM NaCl, 1x Complete EDTA-free Protease inhibitor cocktail (Roche) and 1x PhosSTOP Phosphatase inhibitor cocktail (Roche)]. For figure 6E, similar quantities (about 10 µl pellets) of 0 to 6 hrs old embryos from the indicated genotypes per experimental condition were bleach-dechorionated and washed in Embryo Washing Buffer (0.04% NaCl and 0.03% Triton), and then homogenized on ice and lysed for 30 min at 4°C in 500 µl of Embryo Lysis Buffer [50 mM Tris-HCl pH 7.4, 2 mM EDTA, 150 mM NaCl, 0.1% NP40, 1mM DTT, 1x Complete EDTA-free Protease inhibitor cocktail (Roche) and 2x PhosSTOP Phosphatase inhibitor cocktail (Roche)]. For figure 6G, the cells treated with DMSO or ZM447439 were centrifugated, resuspended in 1ml of Embryo Lysis Buffer, and sonicated. Homogenates were clarified via two rounds of microfuge centrifugation for 15 min at 4°C and then incubated with washed GFP-TrapR-M beads under gentle rotation at RT for 1hr. After magnetic separation, the pellets were washed twice in IP Washing Buffer, resuspended in 50 µl of Laemmli buffer and denatured at 95°C for 10 min and finally bound proteins were recovered

from the beads by magnetic separation.

10 µl of these GFP-IP-enriched proteins were fractionated on 4-15% gradient mini-protean TGX precast gels (Biorad) and electrotransferred using Trans-Blot Turbo mini nitrocellulose transfer packs (Biorad). The membranes were blocked for 2 hrs at RT in blocking buffer [TBS, 0.1% Tween 20, 5% BSA and 1x PhosSTOP Phosphatase inhibitor cocktail (Roche)] and incubated overnight at 4°C in the same buffer (fresh with 1x PhosSTOP) containing primary antibodies at the following dilutions: anti-pS157-CycB at 1:1,000 and a rabbit antitotal CycB antibody (Whitfield et al., 1990) (a kind gift from David M. Glover) at 1:2,000.
After three washes in TBS-T (TBS, 0.1% Tween 20), membranes were incubated for 1 h with the secondary antibody in blocking buffer (fresh with 1x PhosSTOP for anti-pS157-CycB) containing a peroxydase-conjugated anti-rabbit IgG (Jackson Immunoresearch) diluted at 1:10,000. After three washes in TBS-T, bands were detected with the SuperSignal West Pico Chemiluminescent Substrate (Pierce) and visualized using a mini-LAS-4000 Imaging System (Fujifilm).

For the λ-phosphatase experiments, IP on embryos was performed as above, until the washing of the pellet (beads+IP). The pellet was then divided in two: half of it was treated 20 min at 30°C with λ-phosphatase into λ-protein phosphatase buffer (Biolabs), 200 units in 60ul, while the second half was not. The pellets were then resuspended in 50 λl of Laemmli buffer and denatured at 95°C for 10 min and finally bound proteins were recovered from the beads by magnetic separation.

Quantification and Statistics

The number of cell per egg chamber was quantified on DAPI and Rhodamin-phalloidin stained ovaries. We counted the number of nuclei with the DAPI staining. In addition, the number of ring canals stained by Phalloidin was counted for the oocyte so that chambers formed of 32 cells having 2 oocytes with 4 ring canals each (due to encapsulation defects) are not included. Chi-square tests were used to compare the proportions of egg chambers having 8, 16 or 32 cells.

To test if the observed number of pairs of 8-cell cysts was higher than the expected number of pairs if the distribution of 8-cell cysts was random in *aurB*^{1689} homozygous mutant egg chambers, we used the hypergeometric law. We counted 500 *aurB*^{1689} mutant egg chambers in synchronized and aged females. In these conditions, the frequency of 8-cell cyst is lower than in young females (the lower the frequency the more statistically significant becomes a shift in the distribution); and we obtained 27 cysts with 8 cells (percentage p= 27/500= 0.054). We determined the number of cells per cysts (8 or 16) in 4 consecutive egg chambers in each ovariole. This experiment is equivalent to selecting randomly 4 egg chambers without replacement in a population of 500; and each 8-cell cyst being labeled as a success. It is a hypergeometric experiment, and the probability of selecting k egg chambers with 8 cells every 4 egg chambers in a population of 500 egg chambers including 27 egg chambers with 8 cells and 473 with 16 cells, is given by the hypergeometric function:
$P(x=k) = C^{k}_{27} \times C^{4-k}_{473} / C^{4}_{500}$. If the distribution of 8-cell cysts is random in the 500 population, the probability to draw 2 or more 8-cell cysts in one ovariole (i.e. 4 egg chambers in the same ovariole) is $P(x\geq2) = 1 - (P(x=0) + P(x=1)) = 0,016$ (1,6%). We actually observed 6 ovarioles out of 125 (= 6 /125= 0,048) with more than 2 egg chambers with 8 cells. 0,048 is statistically different from 0,016 with $p<0,005$. It demonstrates that the observed frequency of ovarioles with at least 2 cysts with 8 cells is much higher than expected if the 8-cell cysts were randomly distributed in the population of ovarioles. It suggests that appearances of two 8-cell cysts in the same ovariole are not independent, and that it may have a common cause, that we interpret as being a single precursor.

Microscopy

Acquisition of Z-stacks on fixed sample was carried out on Zeiss LSM710 or LSM780 confocal microscopes. For quantification of egg chambers with 8, 16 or 32 cells, ovaries were analyzed with a Upright Widefield Leica Microscope.

For live imaging of larval neuroblasts in figures 2 and S1, brains were mounted in Schneider medium supplemented with 5% serum. Cells were imaged using a Spinning Disk Confocal System Andor Revolution XD (ANDOR Technology, UK). Time-lapse images were then

treated with the microscope software IQ 1.7 (ANDOR Technology, UK) and Fiji.

For live imaging of germarium in figure 4, 7, S1 and S6 ovaries were dissected and mounted in oil (10S, Halocarbon, Sigma) and were imaged with an inverted Confocal Spinning Disk Roper/Nikon equipped with a CDD camera CoolSnap HQ2. Time-lapse images were then treated with Fiji.

For time-lapse phase-contrast microscopy of Hela cells, cells were plated on 35mm glass dishes (CELLview, Greiner bio-one) and put in an open chamber (Life Imaging) equilibrated in 5% CO2 and maintained at 37¢XC. Time-lapse sequences were recorded every 10 or 12 min for 24 h on a Nikon Eclipse Ti inverted microscope with a X20 0.45 NA Plan Fluor ELWD objective lens controlled by Metamorph 6.1 software (Universal Imaging). This microscope was equipped with a cooled CCD camera (HQ2; Roper Scientific). Time-lapse images were then treated with Fiji.

For the photo-activation experiment, ovaries were dissected and mounted in oil (10S, Halocarbon, Sigma). Photo-activation was done with a 2-photon laser at 820nm (3 iterations, laser power 6%, scan speed = 6; these numbers are rough approximations for the excitation power). Imaging was done with a confocal microscope Zeiss LSM 710.

SUPPLEMENTAL REFERENCES

Adams, R.R., Maiato, H., Earnshaw, W.C., and Carmena, M. (2001). Essential roles of Drosophila inner centromere protein (INCENP) and aurora B in histone H3 phosphorylation, metaphase chromosome alignment, kinetochore disjunction, and chromosome segregation. J Cell Biol 153, 865-880.

Basto, R., Brunk, K., Vinadogrova, T., Peel, N., Franz, A., Khodjakov, A., and Raff, J.W. (2008). Centrosome amplification can initiate tumorigenesis in flies. Cell 133, 1032-1042.

Bopp, D., Horabin, J.I., Lersch, R.A., Cline, T.W., and Schedl, P. (1993). Expression of the Sex-lethal gene is controlled at multiple levels during Drosophila oogenesis. Development 118, 797-812.

Brand, A.H., and Perrimon, N. (1993). Targeted gene expression as a means of altering cell fates and generating dominant phenotypes. Development 118, 401-415.

Brandeis, M., Rosewell, I., Carrington, M., Crompton, T., Jacobs, M.A., Kirk, J., Gannon, J., and

Hunt, T. (1998). Cyclin B2-null mice develop normally and are fertile whereas cyclin B1-null mice die in utero. Proc Natl Acad Sci U S A 95, 4344-4349.

Byers, T.J., Dubreuil, R., Branton, D., Kiehart, D.P., and Goldstein, L.S. (1987). Drosophila spectrin. II. Conserved features of the alpha-subunit are revealed by analysis of cDNA clones and fusion proteins. J Cell Biol 105, 2103-2110.

Chen, D., and McKearin, D.M. (2003). A discrete transcriptional silencer in the bam gene determines asymmetric division of the Drosophila germline stem cell. Development 130, 1159-1170.

Chou, T.B., and Perrimon, N. (1992). Use of a yeast site-specific recombinase to produce female germline chimeras in Drosophila. Genetics 131, 643-653.

Giet, R., and Glover, D.M. (2001). Drosophila aurora B kinase is required for histone H3 phosphorylation and condensin recruitment during chromosome condensation and to organize the central spindle during cytokinesis. J Cell Biol 152, 669-682.

Hacker, U., Nystedt, S., Barmchi, M.P., Horn, C., and Wimmer, E.A. (2003). piggyBac-based insertional mutagenesis in the presence of stably integrated P elements in Drosophila. Proc Natl Acad Sci U S A 100, 7720-7725.

Hanyu-Nakamura, K., Kobayashi, S., and Nakamura, A. (2004). Germ cell-autonomous Wunen2 is required for germline development in Drosophila embryos. Development 131, 4545-4553.

Hawkins, N.C., Thorpe, J., and Schupbach, T. (1996). Encore, a gene required for the regulation of germ line mitosis and oocyte differentiation during Drosophila oogenesis. Development 122, 281-290.

Jacobs, H.W., Knoblich, J.A., and Lehner, C.F. (1998). Drosophila Cyclin B3 is required for female fertility and is dispensable for mitosis like Cyclin B. Genes Dev 12, 3741-3751.

Karpova, N., Bobinnec, Y., Fouix, S., Huitorel, P., and Debec, A. (2006). Jupiter, a new Drosophila protein associated with microtubules. Cell Motil Cytoskeleton 63, 301-312.

Lee, T., and Luo, L. (2001). Mosaic analysis with a repressible cell marker (MARCM) for Drosophila neural development. Trends Neurosci 24, 251-254.

Li, Y., Minor, N.T., Park, J.K., McKearin, D.M., and Maines, J.Z. (2009). Bam and Bgcn antagonize Nanos-dependent germ-line stem cell maintenance. Proc Natl Acad Sci U S A 106, 9304-9309.

Martins, T., Maia, A.F., Steffensen, S., and Sunkel, C.E. (2009). Sgt1, a co-chaperone of Hsp90 stabilizes Polo and is required for centrosome organization. EMBO J 28, 234-247.

McKearin, D., and Ohlstein, B. (1995). A role for the Drosophila bag-of-marbles protein in the differentiation of cystoblasts from germline stem cells. Development 121, 2937-2947.

Murray, M.J., and Saint, R. (2007). Photoactivatable GFP resolves Drosophila mesoderm migration behaviour. Development 134, 3975-3983.

Ni, J.Q., Zhou, R., Czech, B., Liu, L.P., Holderbaum, L., Yang-Zhou, D., Shim, H.S., Tao, R., Handler, D., Karpowicz, P., et al. (2011). A genome-scale shRNA resource for transgenic RNAi in Drosophila. Nat Methods 8, 405-407.

Nizak, C., Martin-Lluesma, S., Moutel, S., Roux, A., Kreis, T.E., Goud, B., and Perez, F. (2003). Recombinant antibodies against subcellular fractions used to track endogenous Golgi protein dynamics in vivo. Traffic 4, 739-753.

Perdigoto, C.N., Schweisguth, F., and Bardin, A.J. (2011). Distinct levels of Notch activity for commitment and terminal differentiation of stem cells in the adult fly intestine. Development 138, 4585-4595.

Schuh, M., Lehner, C.F., and Heidmann, S. (2007). Incorporation of Drosophila CID/CENP-A and CENP-C into centromeres during early embryonic anaphase. Curr Biol 17, 237-243.

Spradling, A.C., Stern, D., Beaton, A., Rhem, E.J., Laverty, T., Mozden, N., Misra, S., and Rubin, G.M. (1999). The Berkeley Drosophila Genome Project gene disruption project: Single P-element insertions mutating 25% of vital Drosophila genes. Genetics 153, 135-177.

Van Doren, M., Williamson, A.L., and Lehmann, R. (1998). Regulation of zygotic gene expression in Drosophila primordial germ cells. Curr Biol 8, 243-246.

Whitfield, W.G., Gonzalez, C., Maldonado-Codina, G., and Glover, D.M. (1990). The A- and B-type cyclins of Drosophila are accumulated and destroyed in temporally distinct events that define separable phases of the G2-M transition. EMBO J 9, 2563-2572.

Xu, T., and Rubin, G.M. (1993). Analysis of genetic mosaics in developing and adult Drosophila tissues. Development 117, 1223-1237.

Yue, L., and Spradling, A.C. (1992). hu-li tai shao, a gene required for ring canal formation during Drosophila oogenesis, encodes a homolog of adducin. Genes Dev 6, 2443-2454.